Institute of Experimental Morphology, Pathology and Anthropology with Museum
Bulgarian Anatomical Society

Acta Morphologica et Anthropologica, 30 (3-4)
Sofia ● 2023

Atrophic Age-Related Changes in Cerebral Hemispheres: Euclidean Geometry Based Morphometry of MRI Brain Scans

Nataliia Maryenko, Oleksandr Stepanenko*

Department of Histology, Cytology and Embryology, Kharkiv National Medical University, Kharkiv, Ukraine

*Corresponding author e-mail: maryenko.n@gmail.com, ni.marienko@knmu.edu.ua

The aim of the present study was to conduct a comprehensive morphometric analysis of two-dimensional MRI brain images and determine the simple morphometric parameters of the cerebral hemispheres that best characterize quantitatively brain atrophic changes in normal aging. This study analyzed MRI brain scans from 100 apparently healthy individuals (44 males and 56 females) aged 18 to 86 years (mean age 41.72±1.58 years). For each brain investigation, five tomographic sections were selected, including four coronal and one axial. The perimeter, area values, and their derivative indices were determined. The study has shown that the parameter most sensitive to aging changes was the ratio of two area values: the area corresponding specifically to cerebral tissue and the area that captures the cerebral tissue and the sulcal content. The results of the present study can be used in clinical practice for the quantitative assessment of age-related atrophic changes in cerebral hemispheres.

Key words: aging, brain, cerebral hemispheres, morphometry, neuroimaging

Introduction

Throughout an individual's lifespan, atrophic changes may occur in various brain structures. Age-related alterations in cerebral hemispheres encompass the smoothing of the cerebral surface, the widening and deepening of sulci, a reduction in overall size, and the simplification of gyral shape [1-3, 5, 8, 9, 11, 13]. Atrophic brain changes can result from either normal or pathological aging processes. Notably, changes arising from neurodegenerative conditions, including Alzheimer's disease, can closely resemble those observed in the process of normal brain aging [4, 6, 7, 12]. Consequently, the ability to differentiate between normal and pathological brain aging holds considerable significance in clinical practice.

Currently, in clinical neuroimaging, the detection and characterization of brain atrophic changes are primarily descriptive and subjective. To enhance objectivity and facilitate the quantitative characterization of identified atrophic changes, various morphometric methods are employed, often drawn from classical morphology. In studies aiming to characterize atrophic changes in cerebral hemispheres quantitatively, the following parameters were utilized: volumes of gray and white matter [1-3, 8, 9, 11, 13], cortical thickness [3, 5, 8, 13], gyrification index (defined as the ratio of the total area of the cortical sulcal surface to the superficially exposed area of the cerebral hemispheres) [3, 5, 13], sulcal depth [3, 13], folding area [3], and fractal dimension [3-5, 8]. The morphometric determination of these parameters (except for fractal dimension) derives from Euclidean (traditional) geometry.

However, most of these parameters were determined using the analysis of three-dimensional magnetic resonance imaging (MRI) brain models. In clinical practice, two-dimensional MRI images are assessed for diagnostic purposes, and constructing three-dimensional brain models is not always feasible or practical. Therefore, simplified morphometric approaches are still required for their easy integration into clinical practice. Given this, our aim was to conduct a comprehensive morphometric analysis of two-dimensional MRI brain images and determine the simple morphometric parameters of the cerebral hemispheres that best characterize quantitatively brain atrophic changes in normal aging.

Material and Methods

This study analyzed MRI brain scans from 100 apparently healthy individuals (44 males and 56 females) aged 18 to 86 years (mean age 41.72±1.58 years). The participants of the study underwent diagnostic MRI brain scanning. The inclusion criterion was age 18 years and older. The patients with the presence of pathological structural changes in the brain and surrounding tissues were excluded from the study. Therefore, MRI data from patients who showed no evident brain pathology upon examination were considered relatively normal and were used in the present study. The study was conducted in accordance with the Declaration of Helsinki, and approved by the Commission on Ethics and Bioethics of Kharkiv National Medical University (No. 10 of Nov. 7, 2018) for studies involving humans. Written informed consent has been obtained from the participants of the study.

The MRI images were obtained using a Siemens Magnetom Symphony magnetic resonance scanner with a 1.5 Tesla magnetic induction and a 5 mm section thickness. Both T2 and FLAIR modes were employed. The digital MRI images had a spatial resolution of 72 pixels per inch, with an absolute image scale of 3 pixels = 1 mm.

For each brain investigation, we selected five tomographic sections, comprising four in the coronal (frontal) projection and one in the axial (horizontal) projection. These sections were chosen based on easy identification through anatomical landmarks and their correspondence to various regions of the cerebral hemispheres. The first coronal tomographic section (coronal 1) was located at the level of the anterior points

of the temporal lobes. The second (coronal 2) was at the level of the mammillary bodies. The third (coronal 3) was positioned at the level of the quadrigeminal plate. Due to the section thickness of 5 mm, coronal sections often captured both rostral and caudal colliculi; in cases where different tomographic sections captured either the rostral or caudal colliculi, the section with the well-recognizable rostral colliculi was selected. The fourth (coronal 4) section was located at the level of the splenium of the corpus callosum. The axial section was located at the level of the thalamus. Importantly, these sections corresponded to frequently observed sites of pathological changes in neurodegenerative diseases, including Alzheimer's disease [4].

After the selection of the tomographic sections, we provided morphometry using Adobe Photoshop CS5 software. In each image, we determined the perimeter (P), area (A), and derived indices based on them. To determine the perimeter and area, we employed the "selection" and "analysis" tools. We determined these values in two different ways (**Fig. 1A** and **B**). In the first approach (**Fig. 1A**), we outlined the tomographic sections based on their external (visible) surface, disregarding the sulci. This resulted in the perimeter (P_A), which corresponded to the contour of the visible surface of the cerebral hemispheres, and the area (A_A), representing the overall brain tissue, including the sulci content.

In the second approach (**Fig. 1B**), we outlined the entire pial surface on the tomographic sections, taking the sulci into account. This yielded the perimeter (P_B), corresponding to the contour of the pial surface of the cerebral hemispheres (including the contour inside sulci), and the area (A_B), representing the overall brain tissue (excluding the sulci content).

In addition, we computed several derived indices. Based on the perimeter and area values obtained using two different approaches, we calculated perimeter-to-area ratios (P_A/A_A and P_B/A_B) and shape factors (SF_A and SF_B). The shape factor was determined using the formula: $SF = (4\pi \times A)/P^2$ [10]. Furthermore, we computed the ratio of perimeter values (P_B/P_A) and the ratio of area values (A_B/A_A). The ratio of the two perimeters (P_B/P_A) can be considered a two-dimensional analogue of the gyrification index, as it quantifies the ratio of the total contour length of the cerebral hemispheres' surface to the length of the contour of their superficially exposed surface.

Statistical data processing was performed using Microsoft Excel 2016. Data underwent variation statistics analysis, calculating arithmetic mean (M), standard error (m), minimum (min), and maximum (max) values. The significance of statistical differences between morphometric parameters determined in different tomographic sections was assessed using the Kruskal–Wallis H test and post-hoc Dunn's test with Bonferroni adjustment for multiple comparisons. Interrelationships of the values of the morphometric parameters were assessed using the Pearson correlation coefficient (r) and its significance was evaluated using the Student T test. The significance level for all results was accepted as $p < 0.05$.

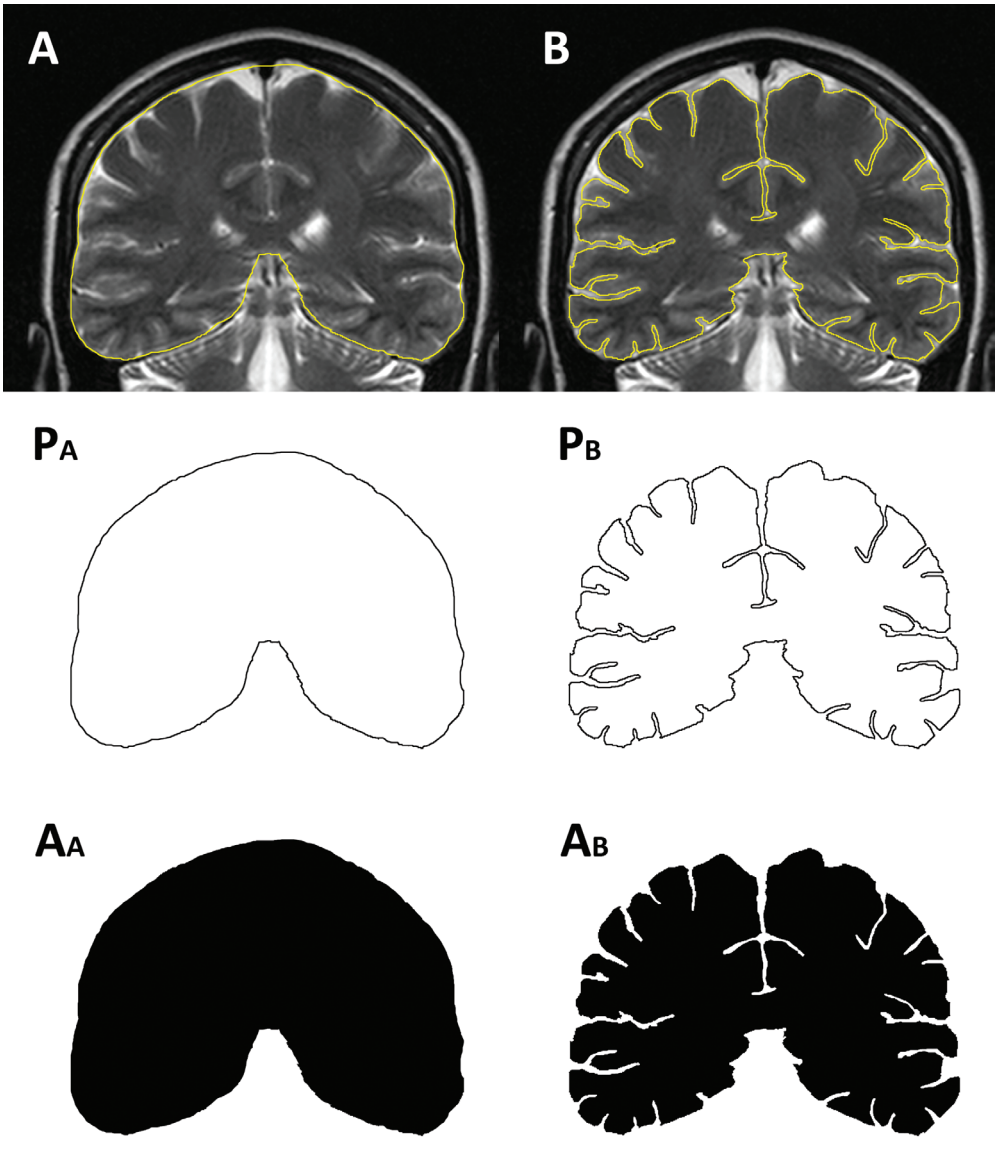

Fig. 1. MRI brain scan of 32 years old female individual, 3rd coronal section. Euclidean geometry based morphometry of cerebral hemispheres: determining area (A_A and A_B) and perimeter (P_A and P_B) values

Results

The descriptive statistics of the morphometric parameters are presented in **Table 1**. When comparing the values determined in different tomographic sections, it was found that the values of all parameters (except for the ratio of perimeters, P_B/P_A) differed

significantly, $p < 0.05$. The post-hoc test has shown that values of the morphometric parameters for the 2nd, 3rd, and 4th coronal sections did not differ significantly from each other. Meanwhile, the values of the 1st coronal section and axial section differed from the values of the 2nd-4th coronal sections. The difference between the values of the 1st coronal and axial sections was significant for all studied parameters except for the shape factor (SF_A) and the ratio of perimeters (P_B/P_A) – these values in the mentioned tomographic sections showed no significant difference. To reveal the peculiarities influencing the values of morphometric parameters, the correlation analysis was provided (**Fig. 2, Fig. 3, Table 2**).

Table 1. The values of the cerebral morphometric parameters

Morphometric parameter		Value	Tomographic section					
			Coronal 1	**Coronal 2**	**Coronal 3**	**Coronal 4**	**Axial**	**Average value**
P_A	Perimeter, cm	M	30.74	45.56	46.26	45.17	57.02	44.95
		m	0.14	0.21	0.20	0.19	0.42	0.17
		min	27.83	41.33	41.73	40.33	50.20	41.16
		max	34.40	50.83	51.90	50.50	72.30	49.49
A_A	Area, cm^2	M	57.24	103.59	103.81	102.17	196.98	112.76
		m	0.62	0.78	0.77	0.79	2.59	0.81
		min	44.97	87.06	87.24	85.31	155.23	93.34
		max	76.56	124.66	128.14	122.24	288.71	131.47
P_A/A_A	Ratio of perimeter and area	M	0.541	0.441	0.447	0.443	0.292	0.433
		m	0.004	0.002	0.002	0.002	0.002	0.002
		min	0.446	0.402	0.378	0.395	0.241	0.390
		max	0.668	0.501	0.502	0.500	0.327	0.479
SF_A	Shape Factor	M	0.760	0.627	0.610	0.629	0.760	0.677
		m	0.004	0.003	0.003	0.002	0.004	0.002
		min	0.605	0.556	0.527	0.565	0.644	0.599
		max	0.824	0.695	0.685	0.675	0.834	0.710
P_B	Perimeter, cm	M	85.69	124.47	128.03	122.64	158.95	123.96
		m	0.93	1.13	1.10	0.98	2.37	0.91
		min	68.67	99.63	107.17	92.07	118.43	102.51
		max	114.07	154.63	153.50	151.83	230.17	149.54

A_B	Area, cm^2	M	47.76	90.17	90.48	90.32	182.85	100.32
		m	0.59	0.77	0.71	0.73	2.35	0.75
		min	36.51	74.10	71.61	73.69	142.69	80.76
		max	65.22	109.88	108.95	109.41	265.36	117.24
P_B/A_B	Ratio of perimeter and area	M	1.809	1.387	1.421	1.363	0.876	1.371
		m	0.020	0.014	0.014	0.012	0.013	0.010
		min	1.379	1.083	1.111	1.088	0.613	1.143
		max	2.286	1.905	1.854	1.792	1.382	1.640
SF_B	Shape Factor	M	0.083	0.075	0.071	0.077	0.095	0.080
		m	0.002	0.001	0.001	0.001	0.002	0.001
		min	0.052	0.046	0.046	0.046	0.046	0.058
		max	0.129	0.112	0.103	0.125	0.163	0.106
P_B/P_A	Ratio of perimeter values (2D gyrification index)	M	2.785	2.732	2.767	2.715	2.788	2.757
		m	0.024	0.022	0.021	0.018	0.035	0.015
		min	2.279	2.211	2.359	2.238	2.148	2.443
		max	3.583	3.464	3.246	3.318	3.881	3.203
A_B/A_A	Ratio of area values	M	0.834	0.870	0.872	0.884	0.929	0.878
		m	0.004	0.003	0.003	0.003	0.002	0.003
		min	0.688	0.755	0.753	0.797	0.821	0.779
		max	0.911	0.923	0.927	0.934	0.955	0.925

The correlation analysis has shown that the values of the morphometric parameters had significant positive correlations when analyzing different tomographic sections (**Fig. 2**). The strongest correlation relationships were observed between adjacent coronal tomographic sections: the 1st and 2nd, 2nd and 3rd, and 3rd and 4th sections. The axial section had moderate to weak relationships with the values of the coronal sections. Considering that morphometric parameters primarily characterize the structural features of the brain, similar anatomical characteristics may influence values in the neighboring regions of the cerebral hemispheres. The parameters that showed the strongest correlations between different tomographic sections were the values of area (A_A and A_B) and their ratio (A_B/A_A).

When analyzing the relationships between different morphometric parameters (**Fig. 3**), it was found that both perimeter values (P_A and P_B), as well as both area values (A_A and A_B), had significant positive correlation relationships with each other in all the studied sections. The values of both perimeter-to-area ratios (P_A/A_A and P_B/A_B), while interrelated by a positive correlation, had negative relationships with most of the studied parameters. The shape factor values (SF_A and SF_B) had weak positive relationships with each other and mainly weak negative relationships with other parameters. The ratio of two perimeters (P_B/P_A), or two-dimensional gyrification index, showed the strongest

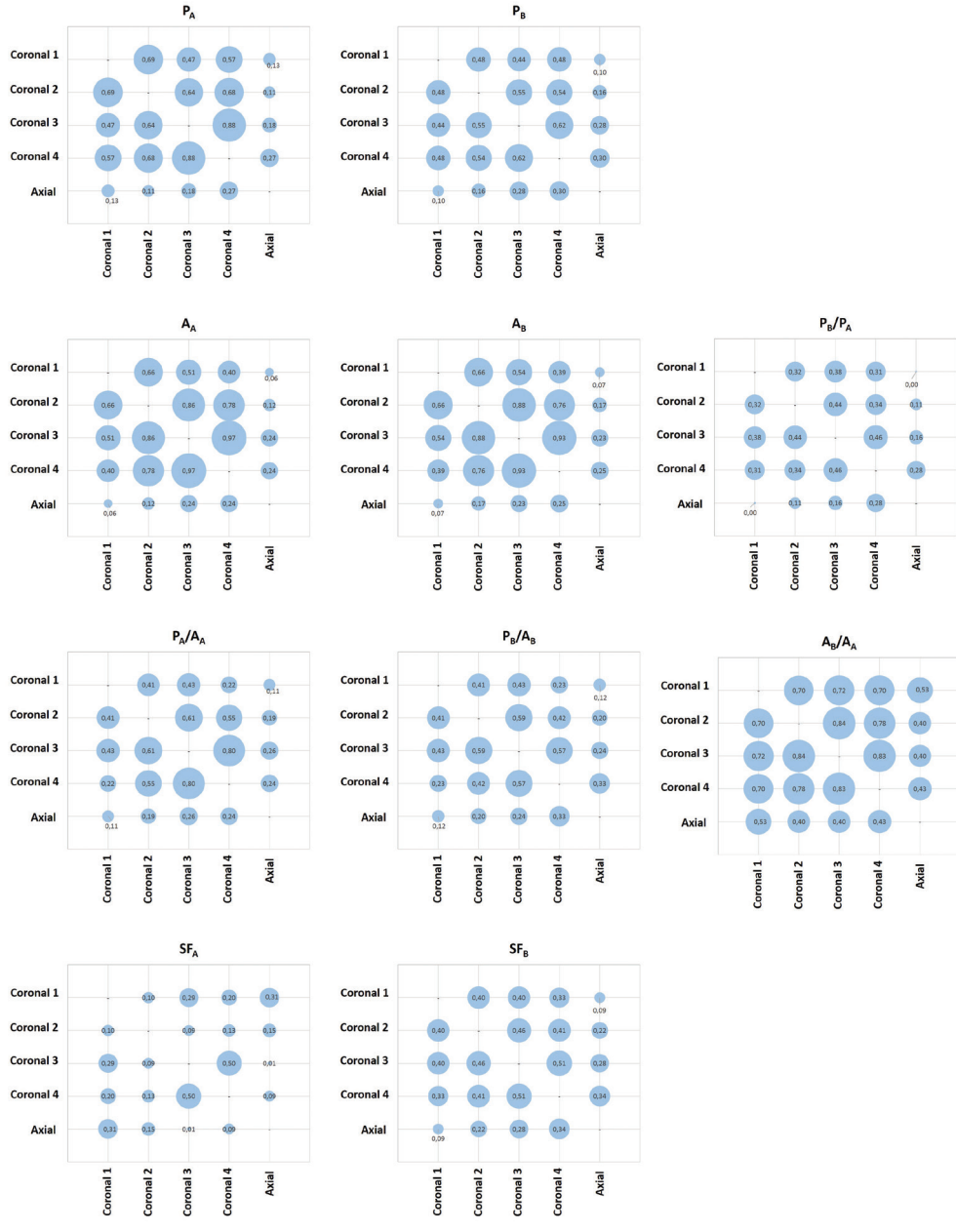

Fig. 2. Correlation relationships of cerebral morphometric parameters of different tomographic sections; the correlation matrix displays the Pearson correlation coefficient (r) values.

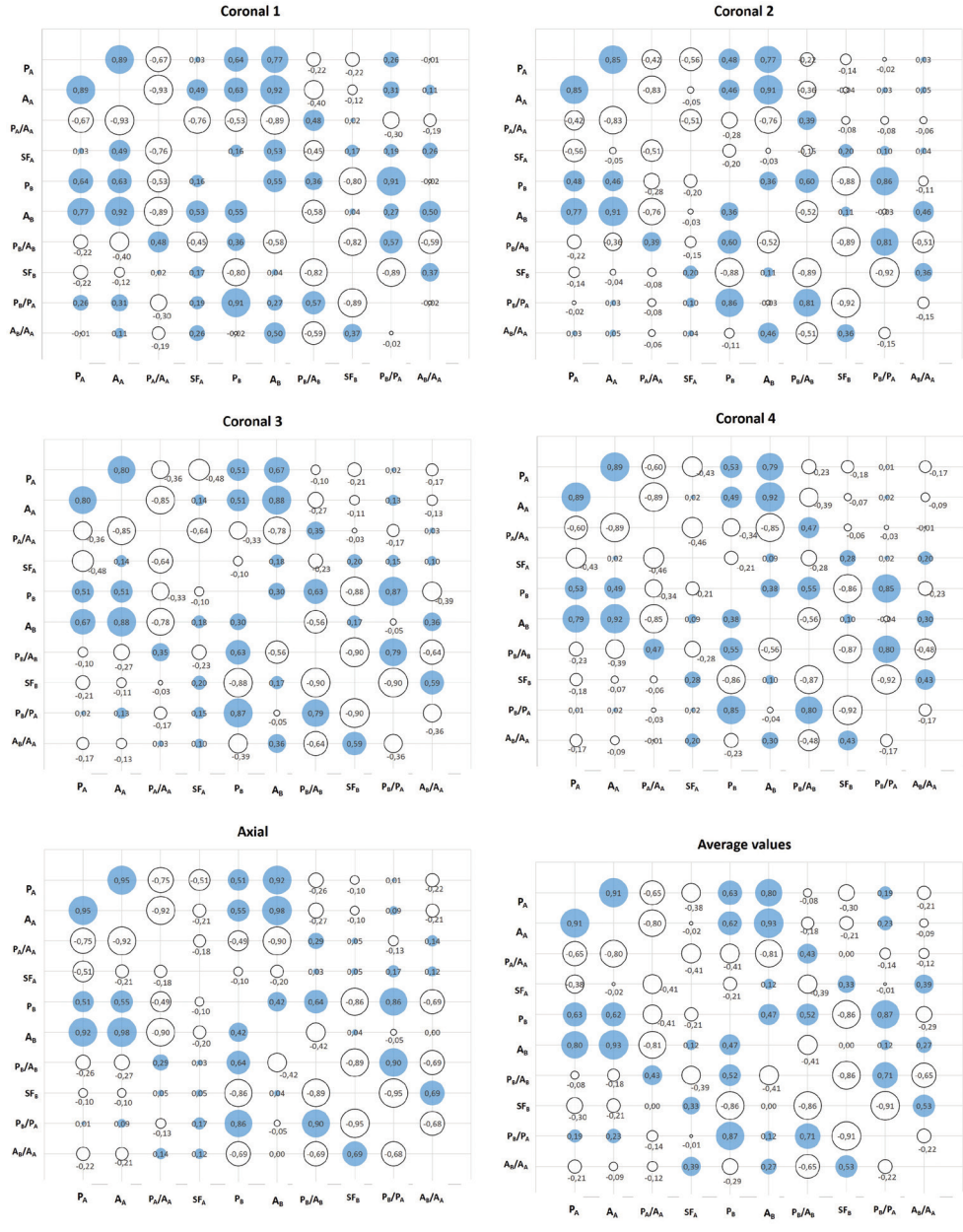

Fig. 3. Correlation relationships of cerebral morphometric parameters; the correlation matrix displays the Pearson correlation coefficient (r) values

relationships with perimeter P_B and the value of P_B/A_B. The ratio of two areas (A_B/A_A) exhibited diverse correlations with other studied parameters.

To identify the parameter that most accurately describes age-related changes, we calculated correlation coefficients between the values of the studied parameters and age (**Table 2**).

Table 2. Correlation coefficients (r) characterizing relationships between cerebral morphometric parameters and age

		Tomographic section					
		Coronal 1	**Coronal 2**	**Coronal 3**	**Coronal 4**	**Axial**	**Average value**
P_A	Perimeter, cm	-0.164	-0.036	0.130	0.090	-0.067	-0.020
A_A	Area, cm^2	-0.191	-0.159	-0.053	0.013	-0.141	-0.159
P_A/A_A	Perimeter-to-area ratio	0.199*	0.247*	0.195	0.058	0.217*	0.260**
SF_A	Shape Factor	-0.111	-0.194	-0.293**	-0.171	-0.180	-0.316**
P_B	Perimeter, cm	-0.232*	-0.171	0.000	-0.104	0.016	-0.104
A_B	Area, cm^2	-0.396***	-0.385***	-0.347***	-0.197*	-0.219*	-0.382***
P_B/A_B	Perimeter-to-area ratio	0.234*	0.172	0.281**	0.088	0.205*	0.290**
SF_B	Shape Factor	-0.027	-0.031	-0.190	-0.030	-0.143	-0.133
P_B/P_A	Ratio of perimeter values (2D gyrification index)	-0.196*	-0.174	-0.073	-0.173	0.065	-0.143
A_B/A_A	Ratio of area values	-0.567***	-0.582***	-0.630***	-0.536***	-0.378***	-0.645***

Note: * – $p<0.05$; ** – $p<0.01$; *** – $p<0.001$

Most of the studied parameters exhibited negative correlation relationships with age, except for both perimeter-to-area ratios (P_A/A_A and P_B/A_B), which showed weak positive correlation relationships. Both perimeter values, as well as both area values, slightly decreased with age, reflecting an overall decrease in brain size during aging. Both shape factor values had weak relationships with age, indicating that the cerebral

shape did not change significantly. An interesting finding is that the two-dimensional gyrification index (P_B/P_A) was not significantly affected by age-related changes.

The strongest negative relationships with age were exhibited by the ratio of area values (A_B/A_A), and these relationships exceeded the relationships exhibited by the area values separately. Considering that the area value A_B has shown a more intensive decrease than the A_A value, we can conclude that the difference between these two areas increases with age. The A_A value captures the entire area of the hemispheres, while the A_B value does not capture the area corresponding to the sulcal content. With the widening and deepening of the sulci during aging, the area occupied by sulcal content increases, and the difference between area values (A_A and A_B) increases in turn. Thus, age-related brain atrophic changes result in a decrease in the space in the cranial cavity filled by the cerebral tissue. Based on this, we can conclude that the ratio of two areas was the most accurate and sensitive parameter among those studied to characterize quantitatively age-related atrophic changes in cerebral hemispheres. We calculated confidence intervals for the A_B/A_A values (**Fig. 4**), which can be used as norm criteria for the assessment of the results of brain morphometry.

Discussion

In this study, we have conducted a comprehensive morphometric analysis focused on selecting the most sensitive parameter for detecting age-related changes. The morphometric assessment of age-related changes in cerebral hemispheres utilizing the morphometric approaches deriving from Euclidean geometry was employed in number of studies. The studies closest to the present one included analyses of the cerebral surface [5, 13] and analyses based on the volumetric indices [1, 2, 8, 9, 11, 13].

The study of F. Zheng et al. [13] has shown age-related decrease in the cortical thickness and local gyrification index as well as a decrease in the gray and white matter volumes ($r^2 > 0.16$). In the study by C.R. Madan and E.A. Kensinger [5], it was noted that certain morphometric parameters exhibited negative correlations with age: mean cortical thickness ($r = – 0.603$) and gyrification index ($r = – 0.494$). Thus, in these studies, it was revealed that the three-dimensional gyrification index decreased with age, while our study has shown weak correlations between age and the two-dimensional gyrification index. This difference in findings can be explained by differences in methodologies: the three-dimensional determination of the gyrification index captures the entire cerebral surface, while the two-dimensional variant characterizes individual tomographic sections.

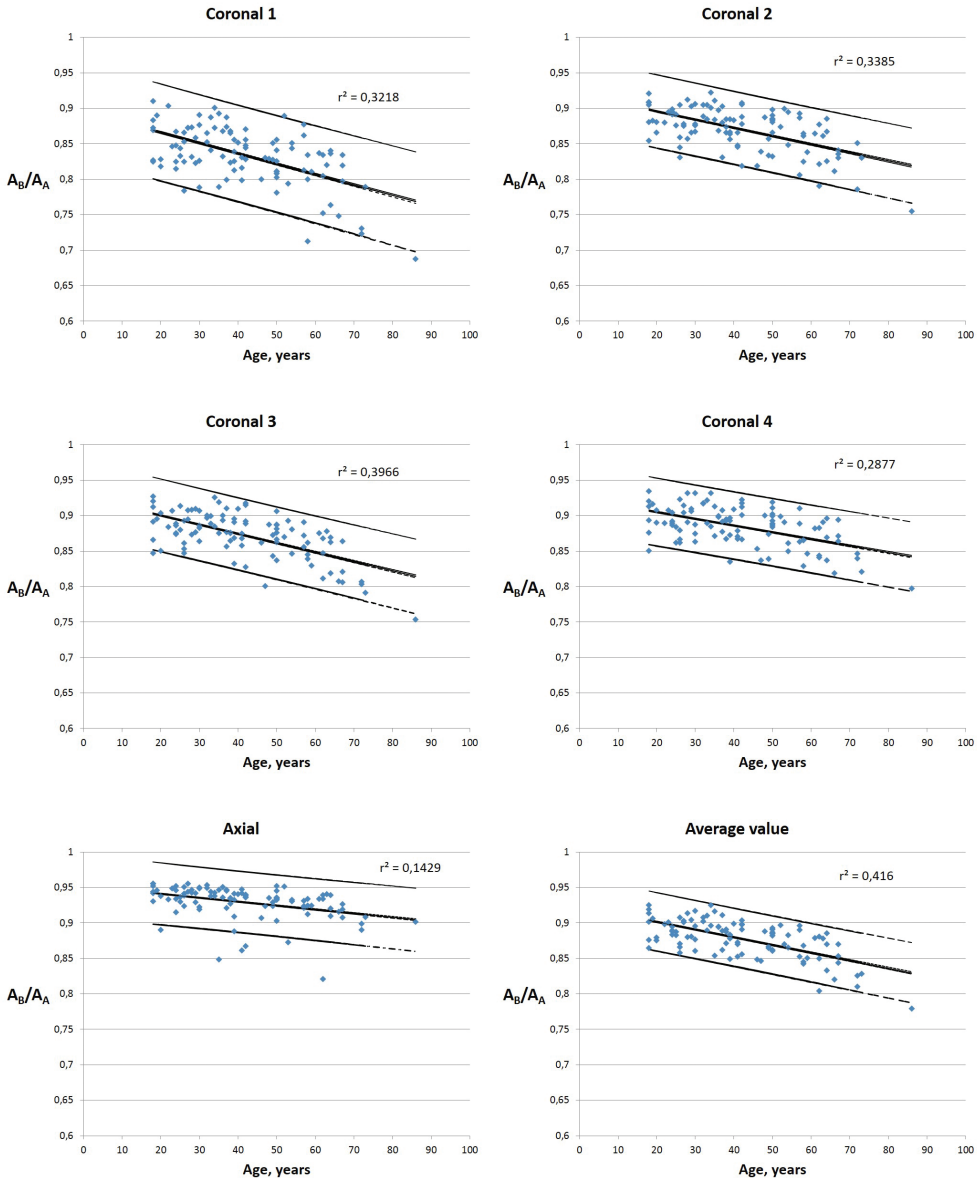

Fig. 4. Age dynamics and confidence intervals of the A_B/A_A values (ratio of area B and area A values)

The studies of Y. Ge et al. [1], R. Riello et al [9], and K. B. Walhovd et al. [11] have demonstrated age-related decrease in the volumes of gray and white matter. The study by P. Podgórski et al. [8] also demonstrated decrease in volumes of total gray matter and white matter; additionally, the study describes decrease in cortical thickness, gyrification index, and increase in the volume of cerebrospinal fluid as

well as sulcal depth. Another volumetric study by C. D. Good et al. [2] demonstrated a significant decrease in gray matter volume ($r^2 = 0.489$), while the decline in white matter volume was considered insignificant by the authors ($r^2 = 0.326$). The authors also revealed an increase in the volume of cerebrospinal fluid ($r^2 = 0.377$).

We did not find in the accessible literature the application of a parameter similar to the ratio of two areas used in the present study. Given that the difference between two area values and their ratio depends mainly on sulcal depth and width, the deepening and widening of sulci in aging lead to an increase in the area ratio (as described in our study), as well as an increase in the volume of cerebrospinal fluid filling the sulci [2, 8]. Thus, the age-related changes in area ratio A_B/A_A correspond to the changes in the volume of cerebrospinal fluid; moreover, both parameters exhibited close values of the correlation coefficient characterizing the relationships with age ($r^2 = 0.416$ and $r^2 = 0.377$ [2], respectively). Therefore, this parameter introduced in the present study may become a useful additional parameter for the quantitative assessment of the atrophic changes in cerebral hemispheres.

Conclusions

The study has shown that the parameter most sensitive to aging changes was the ratio of two area values: the area corresponding to cerebral tissue and the area that captures the sulcal content. The results of the present study can be used in clinical practice for the quantitative assessment of age-related atrophic changes in cerebral hemispheres.

References

1. **Ge, Y., R. I. Grossman, J. S. Babb, M. L. Rabin, L. J. Mannon, D. L. Kolson.** Age-related total gray matter and white matter changes in normal adult brain. Part I: volumetric MR imaging analysis. – *AJNR Am. J. Neuroradiol*., **23**(8), 2002, 1327-1333.
2. **Good, C. D., I. S. Johnsrude, J. Ashburner, R. N. Henson, K. J. Friston, R. S. Frackowiak.** A voxel-based morphometric study of ageing in 465 normal adult human brains. – *NeuroImage*, **14**(1 Pt 1), 2001, 21–36.
3. **Im, K., J. M. Lee, U. Yoon, Y. W. Shin, S. B. Hong, I. Y. Kim, J. S. Kwon, S. I. Kim.** Fractal dimension in human cortical surface: multiple regression analysis with cortical thickness, sulcal depth, and folding area. – *Hum. Brain Mapp.*, **27**(12), 2006, 994-1003.
4. **King, R. D., A. T. George, T. Jeon, L. S. Hynan, T. S. Youn, D. N. Kennedy, B; the Alzheimer's Disease Neuroimaging Initiative.** Characterization of Atrophic Changes in the Cerebral Cortex Using Fractal Dimensional Analysis. – *Brain Imaging Behav*., **3**(2), 2009, 154-166.
5. **Madan, C. R., E. A. Kensinger.** Cortical complexity as a measure of age-related brain atrophy. – *Neuroimage*, **134**, 2016, 617-629.
6. **Matsuda, H.** MRI morphometry in Alzheimer's disease. – *Ageing Res. Rev*., **30**, 2016, 17-24.
7. **Pini, L., M. Pievani, M. Bocchetta, D. Altomare, P. Bosco, E. Cavedo, S. Galluzzi, M. Marizzoni, G. B. Frisoni.** Brain atrophy in Alzheimer's Disease and aging. – *Ageing Res. Rev*., **30**, 2016, 25-48.

8. **Podgórski, P., J. Bladowska, M. Sasiadek, A. Zimny.** Novel Volumetric and Surface-Based Magnetic Resonance Indices of the Aging Brain - Does Male and Female Brain Age in the Same Way? – *Front. Neurol.,* **12**, 2021, 645729.
9. **Riello, R., F. Sabattoli, A. Beltramello, M. Bonetti, G. Bono, A. Falini, G. Magnani, G. Minonzio, E. Piovan, G. Alaimo, M. Ettori, S. Galluzzi, E. Locatelli, M. Noiszewska, C. Testa, G. B. Frisoni.** Brain volumes in healthy adults aged 40 years and over: a voxel-based morphometry study. – *Aging Clin. Exp. Res.,* **17**(4), 2005, 329-336.
10. **Underwood, E. E.** *Quantitative Stereology.* London: Addison-Wesley; 1970.
11. **Walhovd KB, A. M. Fjell, I. Reinvang, A. Lundervold, A. M. Dale, D. E. Eilertsen, B. T. Quinn, D. Salat, N. Makris, B. Fischl.** Effects of age on volumes of cortex, white matter and subcortical structures. – *Neurobiol. Aging*, **26**(9), 2005, 1261-1270; discussion 1275-1278.
12. **Whitwell, J. L.** Alzheimer's disease neuroimaging. – *Curr. Opin. Neurol*., **31**(4), 2018, 396-404.
13. **Zheng, F., Y. Liu, Z. Yuan, X. Gao, Y. He, X. Liu, D. Cui, R. Qi, T. Chen, J. Qiu.** Age-related changes in cortical and subcortical structures of healthy adult brains: A surface-based morphometry study. – *J. Magn. Reson. Imaging,* **49**(1), 2019, 152-163.